X-ray Scattering at Breakout from Warm Dense Iron

Contact swhite06@qub.ac.uk

S. White, B. Kettle, M. Calvert, C.L.S. Lewis and D. Riley
Centre for Plasma Physics, Queen's University Belfast
University Road, Belfast, BT7 1NN, UK

A. Rigby, M. Oliver and G. Gregori
Clarendon Laboratory, University of Oxford
South Parks Road, Oxford, OX1 3PU, UK

E. Tubman, C.D.M. Murphy and N. Woolsey
York Plasma Institute, University of York,
Church Lane, Heslington, YO10 5DQ, UK

Introduction

Since 1998[1,2] the study of warm dense matter using x-ray scattering techniques has proven to be a valuable technique for characterization of these dense, transient plasma states. Considerable interest has been focused on the study of relatively light elements such as hydrogen and lithium, up to carbon. Carbon and hydrogen are interesting in particular as they are thought to be present, under warm dense conditions, in the cores of Jovian mass planets. However there is major motivation to extend research to heavier elements such as iron as not only is it thought to be present in the core of earth and the rocky planets of our own solar system but many so called super earths which have recently been discovered[3,4,5]. Accurate planetary modeling will require an in depth understanding of how iron behaves under the extreme temperatures and pressures at the heart of an Earth mass planet.

At the inner/outer core boundary of Earth iron is thought to be present at a temperature of roughly 7000K and a pressure of about 330GPa, roughly 3 million times atmospheric pressure. Under such immense pressure the density of iron increases to about 13g/cc, 1.65 times solid density.

The most common method for producing samples under these conditions has been to use laser produced shocks to heat and compress the material. Using this method, it is incredibly difficult to produce uniform samples of material for x-ray probing. This experiment has used two techniques to improve the target uniformity. Firstly we have exploited the temporal shaping capability now available on the shock drive laser beam at TAW using the shaped long pulse oscillator. Secondly we have used a modification on the traditional scattering geometry.

Previous experiments[6,7,8] have shocked the sample target using single sided irradiation. The probe x-rays have then been incident upon the same side and the scattered radiation is observed through the target. This means that the whole target is being probed, which puts restrictions upon the target thickness. The maximal scatter signal is observed when the target is an attenuation depth thick, typically about 10µm. Any deviation from this leads to a rapid loss in scatter signal.

For our experiment we still irradiate from a single side, but now we probe the rear surface of the target with x-rays and observe the light scattered back out through the same surface. This has a few advantages. Since our scatter diagnostics are placed behind the target we see a reduction in background noise due to the hot plasma created by the shock beams. Secondly, since the light escapes through the same target surface it is incident upon we no longer have a restriction on target thickness, as the target thickness increases we will observe increased scatter signal until the thickness is effectively infinitely thick. Provided we can drive a shock through the target we are free to choose an increased thickness.

Figure 1 a) & b) shows results from hydrodynamic simulations for these two experiment designs. The simulations were performed using HYADES[9], a 1-D radiation hydrodynamics model. Both images show snapshots of the target conditions just as the shock wave has reached the rear surface, i.e. at the shock breakout. For easier comparison position has been shown as distance from the rear of the target. Both conditions have used the same laser drive, a 1.5ns flat top pulse with 200ps rise and fall times. The peak intensity was $3x10^{13}$ W/cm^2.

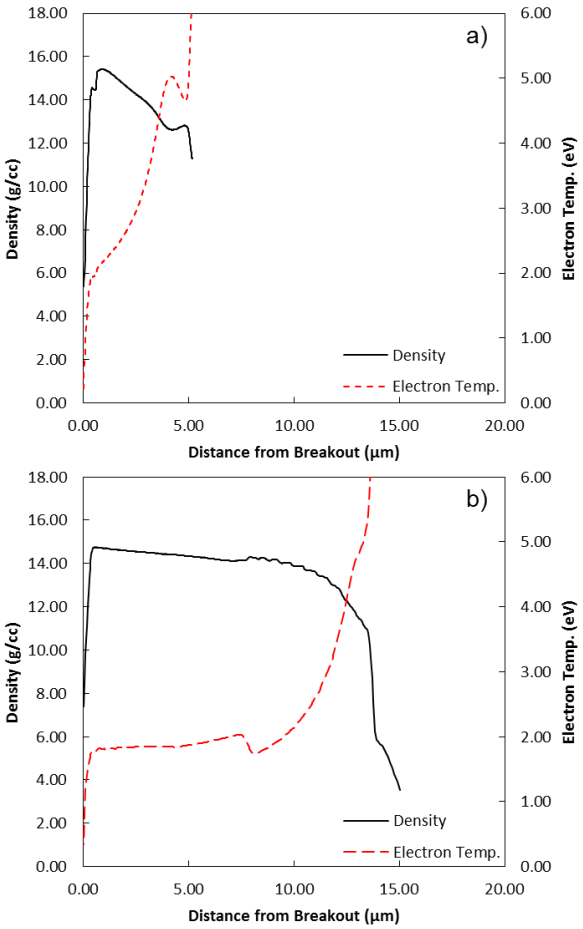

Figure 1. Comparison of hydrodynamic conditions for both experiment geometries.

Figure 1 a) shows results for the conventional geometry. A 10µm iron foil was used with a 4.5µm plastic ablator. As the scatter is observed in transmission the conditions throughout the whole target must be considered. The density and temperature were

13.8±1.4g/cc and 3.3±1.2eV. Figure 1 b) shows the conditions for the current experiment design. A 25µm thick iron foil was used with the same plastic ablator. In this geometry the scattered x-rays which escape only penetrate up to about 8µm deep into the target, in fact over 95% of the scatter signal should come from within this region. The corresponding density and temperature is 14.3±0.8g/cc and 1.9±0.2eV. Target uniformity has greatly increased as well as an improvement in the target conditions. The increased density and decreased temperature provides a more suitable WDM sample.

Experimental Set-Up

The experiment was carried out in Target Area West (TAW) of the Vulcan laser facility. The ns long pulse beams were used to drive a shock through our iron sample targets. One of the CPA beams available in TAW was used to produce a bright back lighter source of Vanadium He_α x-rays.

The shock drive beams were frequency doubled to 527 nm using 12 mm thick KDP crystals in type II configuration. The shaped long pulse oscillator was used to deliver, after conversion, a quasi-flat topped pulse about (1 to 2) ns long. On every shot leakage from one of the long pulse beams was captured using a fast diode (about 100ps rise time) and a 6 GHz oscilloscope to measure the shock drive temporal profile.

B8 was used as the back lighter beam. To improve conversion of laser light to x-rays we used a 270 mm square, 9.5mm thick KDP crystal, large enough to accommodate the full aperture of the beam, to frequency double B8. We used a pulse duration of (50 to 100) ps. The final optic was an f/3 OAP which we defocused to obtain a (100 to 200) µm focal spot OAP. Due to the possibility of damaging the gratings we were limited to 150 J of infrared energy before the compressor. Assuming that the calorimeters we used have a precision of ± 5 %, the compressor throughput was measured on the experiment to be 83 ± 4 %. The crystal conversion efficiency was measured as 57 ± 4 %. This results in ≈ 60 J energy on target at an intensity of $\approx 5 \times 10^{15}$ W/cm^2.

Targets were supplied by CLF's target fabrication group. The sample target was a 25 µm iron layer coated with 4.5 µm of plastic (Parylene-N - C_8H_8). Hybrid phase zone plates (HZP's) placed about 10cm after f=1m, f/10 lenses were used to make a smooth, (1.4 × 0.9) mm diameter, flat top elliptical focal spot. The focal spot dimensions were chosen to match the area probed by the majority of the vanadium He_α x-rays. The energy on target could be easily varied by firing between 2 and 6 of the long pulse beams giving intensities of about 3×10^{13} W/cm^2.

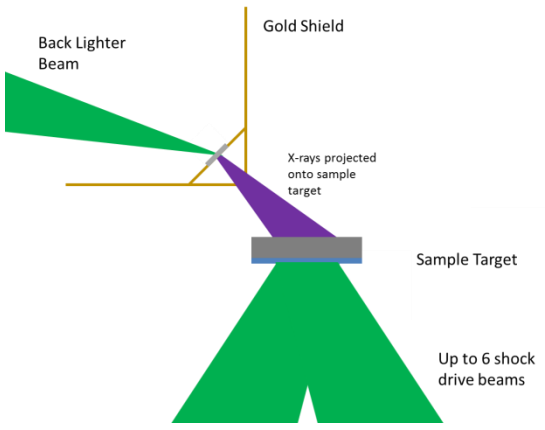

Figure 2. Schematic of Experiment

The back lighter target consisted of a 5 µm thick vanadium foil mounted over a 1 mm hole in the base of a gold cone. The walls of the gold cone are 50 µm thick which will effectively block (transmission<0.1%) all sub 20 keV x-rays. Even at 30 keV the transmission will be less than 1%. This is absolutely necessary to block the direct lines of sight between the back lighter and scatter diagnostics. The detectors used with the scatter diagnostics are not sensitive to photons above about 25 keV. The tip of the gold cone was removed to form a pinhole 250 µm in diameter placed 1.5 mm from the vanadium foil. The sample target was placed a further 3.5mm from the pinhole. This arrangement meant that the x-rays would be projected onto a uniformly heated elliptical area of the sample target.

X-rays elastically scattered by the sample target were collected using three separate HOPG crystal spectrometers coupled to Andor DX420-BN CCDs. The crystals consisted of cylindrically curved glass substrates 30 mm wide, 20 mm long (along the cylinder axis), with a radius of curvature of 50 mm, coated in >150 µm of grade ZYA HOPG, i.e. HOPG possessing a mosaic spread of 0.4° ± 0.1°.

We attempted to set-up a VISAR diagnostic for the sample target. Though we were unable to get high contrast fringes from the rear of the target we were able to use the 'blanking' property of the probe laser light on shock breakout to see when the shock broke out. The probe laser we used was an injection seeded Powerlite Continuum ND:YAG Q-switched laser. The seeding option was necessary to have sufficient temporal resolution for use in a VISAR system. The output of the laser was about 1J at 532nm in a 6ns Gaussian temporal profile. We attenuated the pulse by ND 3 before injecting into a 1mm core optical fiber which transported the beam to the VISAR imaging line.

It was absolutely crucial that the probe x-rays arrived at the rear of the sample target within a few 10s of ps of the shock breaking out. Too early and predominantly cold material would be probed. Too late and the target would have disintegrated significantly into a lower density plasma. Initial timing of the beams was performed using a Hamamatsu C5680 streak camera which belonged to QUB. Synchronisation of the long pulse beams was achieved by scattering light from a paper target which was then imaged onto the streak. The ≈ 1 ns long pulse beams were timed to within ± 25 ps. The jitter between the individual long pulse beams may be considered negligible since all 6 were derived from the same oscillator. Unfortunately the jitter between B8 and the long pulse beams was at least ± 150ps. The limited number of shots as well as some evidence that the mean 'position' of the short pulse can change between days made this number hard to estimate. Because of this it was necessary to set up a fiducial for the short pulse. This was done by picking off a small portion of B7 inside the target chamber. For a fiducial to be practical we need to use the compressed CPA pulse so it must be picked off after the chamber. It was not practical to use B8, however since B7 originates form the same oscillator we may use that as a time reference for B8 as well. A small portion of B8 was relayed and focused onto the VISAR streak camera slit. By scattering laser light from B8 from the sample target position and measuring the delay between B7 and B8 on the VISAR streak we had a time fiducial for B8. By using B7 as the fiducial signal on the streak we were able to run the fiducial on full shots and thus by monitoring the time between B7 and shock breakout we knew at what time the sample was probed.

Experimental Results

Figure 3 shows data collected by one of the three HOPG spectrometers used to collect scattered x-rays. The spectrometer was looking at a scattering angle of 68.6°±6.0°. The range in angle here is due to using 30mm wide crystals at a distance of about 130mm. The red solid line shows a fit to the data. The fit function consisted of two pseudo Voight profiles. One profile to

account for the broad background signal due to broadband x-rays and a second profile describing the scatter signal sitting on top. The red dashed line shows the background profile only. Sample-only, cold, and null shots were taken to verify that the second signal was indeed due to x-rays scattered by heated material.

By using these functions to perform a background subtraction we were able to make estimates for the total integrated counts on the CCD due to elastically scattered x-rays. The counts recorded at each scattering angle were scaled to account for relative differences such as target and filter transmission. The data could not be corrected for crystal reflectivity though as no calibration data currently exists.

We are currently undertaking work to build a test station at Queen's University Belfast (QUB) using a Amptek gold target micro-focus x-ray tube to perform the necessary measurements to calibrate the HOPG crystals.

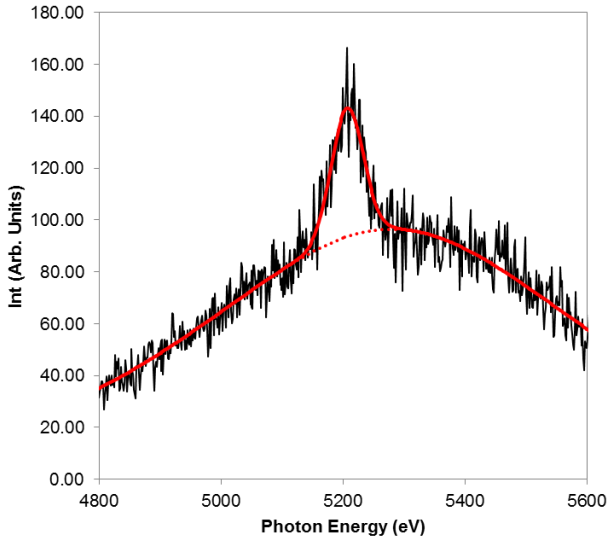

Figure 3. Example of a typical data shot on one of the scattering spectrometers. Data shown here was collected at a scattering angle of 68.6°±6.0°.

A comparison of the measured scattering intensity corrected for all relative differences and a calculation of the scattering cross-section for a sample of iron at 14g/cc and 1.5eV is shown in figure 4. The data set consists of 3 shots each at 68.6°, 90°, and 109.6°, and 4 shots each at 81.0°, 100.0°, and 132.3° degrees. The match between model and experiment at the moment is not great, however this is a preliminary analysis. Also, it is not unreasonable to suspect that the crystal reflectivities could vary by a factor of 2 to 3 between the crystals. Variances in the HOPG crystal's degree of mosaicity, which is sensitive to the manufacturing process, could affect the integrated reflectivity. If for example system 3's crystal was about twice as reflective as the other two it would suggest that the scattering cross-section profile is much steeper than modeling would suggest, and pushed towards higher angle. Motivated by this we are currently building a crystal calibration system, at QUB using an Amptek micro x-ray source.

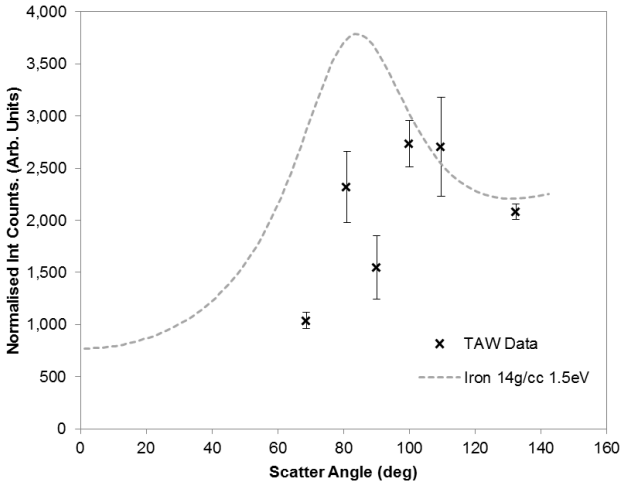

Figure 4. Comparison of experimental results of the scattering power to an estimate based upon calculating the ionic structure factor using an HNC model with a screened Yukawa potential and calculating ionic form factors using the approach of Pauling[7,8].

Conclusions

By observing scatter from the rear of a shocked target we have demonstrated that one can examine much more uniform samples of warm dense matter. This geometry also leads to more flexibility in target design. The results of an experiment utilizing this design have shown promising results. A calibration station utilizing an x-ray micro focus tube is currently being built at QUB and will be used to absolutely calibrate the spectrometers fielded on this experiment. Thus, we will be able to accurately calculate the elastic x-ray scattering cross-section of iron under extreme conditions.

Acknowledgements

The authors wish to acknowledge and thank the staff of the VULCAN laser, engineering, target area, and target fabrication at CLF for their help and support during the experiment.

This work was supported in part by EPSRC grant EP/K000591/1 and by the Science and Technology Facilities Council of the United Kingdom.

References

1. N. C. Woolsey, D. Riley and E. Nardi, Rev. Sci. Instr. **69(2)**, 418-424 (1998)
2. D Riley, NC Woolsey, D McSherry, I Weaver, A Djaoui, and E Nardi, Phys. Rev. Lett. **84(8)**, 1704-1707 (2000)
3. A. Wolszczan, *et al*, Nature, **355**, 154-147 (1992)
4. E. J. Rivera, *et al*, Astrophys. J.**, 634**, 625 (2005)
5. N. Haghighipour, *et al*, Contemporary Physics, **52**, 403-438 (2011)
6. White e*t al*, HEDP, **9**, 573 (2013)
7. Kritcher *et al*, Phys. Rev. Lett. **103**, 245004 (2009)
8. E. García Saiz *et al*, Phys Rev. Lett. **101**, 075003 (2008)
9. J. T. Larsen and S. M. Lane, J. Quant. Spectrosc. Radiat. Transfer, **51,** 179 (1994)
10. L. Pauling and J. Sherman. Zeit. F. Krist, **81**:1-32 (1932)
11. Wünsch *et al*, Phys. Rev. E, **77**, 056404, (2008)